



Research  
Civil Engineering—Article

# Fundamental Issues Towards Unified Design Theory of Recycled and Natural Aggregate Concrete Components



Jianzhuang Xiao <sup>a,b,\*</sup>, Kaijian Zhang <sup>c,a</sup>, Tao Ding <sup>a</sup>, Qingtian Zhang <sup>c,a</sup>, Xuwen Xiao <sup>a</sup>

<sup>a</sup> Department of Structural Engineering, Tongji University, Shanghai 200092, China

<sup>b</sup> College of Civil Engineering and Architecture, Guangxi University, Nanning 530004, China

<sup>c</sup> College of Civil Engineering, Fuzhou University, Fuzhou 350116, China

## ARTICLE INFO

### Article history:

Received 15 July 2022

Revised 10 October 2022

Accepted 21 March 2023

Available online 20 June 2023

### Keywords:

Recycled aggregate concrete (RAC)

Natural aggregate concrete (NAC)

Strength determination

Constitutive relation

Reliability

Unified design theory

## ABSTRACT

In the past 20 years, recycled aggregate concrete (RAC), as a type of low-carbon concrete, has become a worldwide focus of research. However, the design methodology for RAC structural components remains a challenge. Consequently, demands for a unified design of natural aggregate concrete (NAC) and RAC components have been presented. Accordingly, this study analyses the necessity of a unified design theory and provides an in-depth demonstration of the strength determination, compressive constitutive relationship, and design method of concrete components. The coefficient of variation of RAC strength is found to be generally higher than that of NAC strength. The compressive and tensile strengths of RAC can be defined and determined using the same method as that used for NAC. The uniaxial compressive constitutive relationship between NAC and RAC has a unified mathematical expression. However, the elastic modulus of RAC decreases, and its brittleness exhibits an increasing trend compared with that of NAC. Finally, to unify the design formulae of RAC and NAC components for bearing capacity, modification factors for RAC components are proposed considering safety and reliability. Additionally, the feasibility of the proposed unified time-dependent design theory is demonstrated in terms of conceptual design and structural measures considering the effects of strength degradation and reinforcement corrosion. It is believed that this study enriches and develops the basic theory of concrete structures.

© 2023 THE AUTHORS. Published by Elsevier LTD on behalf of Chinese Academy of Engineering and Higher Education Press Limited Company. This is an open access article under the CC BY-NC-ND license (<http://creativecommons.org/licenses/by-nc-nd/4.0/>).

## 1. Introduction

The supply of natural aggregates is gradually failing to satisfy construction demands because of the limited exploitation of natural mines and river sands [1]. In addition, the annual output of construction and demolition wastes has increased obviously in recent years. The resource utilization rate should be increased; therefore, promoting the application of recycled aggregate concrete (RAC) is necessary. Previously, RAC was mainly used in pavement bases, floor cushions, and enclosure structures with low added value. With the increasing demolition of old buildings, the application of RAC structures to gradually replace parts of natural aggregate concrete (NAC) structures is an important future development trend conforming to the requirements of recycling and low-carbon strategies.

Concrete that has been prepared using recycled aggregates is called RAC. In RAC, the natural aggregates are partially (more than 15%) or fully replaced by recycled aggregates [2] produced from waste concrete through crushing and sieving according to a certain gradation. Hence, waste concrete can be recycled into new structural materials, consequently reducing environmental pollution and construction costs and partially replacing NAC as low-carbon materials for infrastructure construction. The economic benefit of RAC can be improved by increasing the replacement ratio [3]. Currently, the recycled materials produced by resource production lines include recycled coarse or fine aggregates and recycled powder [4]. Among these, recycled coarse aggregates have been widely applied to existing concrete engineering structures [5]. The replacement ratio is generally 30%–50% and even reaches 100% in components with special requirements.

It should be noticed that the sources and composition of waste concrete are generally complex. The variability of properties of RAC is quite different from NAC. The properties of RAC are affected by many factors, such as the source of waste concrete, quality,

\* Corresponding author.

E-mail address: [jzx@tongji.edu.cn](mailto:jzx@tongji.edu.cn) (J. Xiao).

gradation, and replacement ratio [6,7], and they degrade when the replacement ratio increases. The compressive strength of RAC decreases with the increasing replacement ratio under the same water–binder ratio; its strength decreases by 20% when the replacement ratio is 100% [8]. Because recycled aggregates are produced through crushing, cleaning, and grading of waste concrete, damage within the material can accumulate during these processes. The recycled aggregate is a multiphase material composed of natural aggregate and attached old mortar [9]. Compared with natural aggregate, recycled aggregate has a higher water absorption and crushing index [10,11]. The old mortar can be reduced by physical means, such as “grinding” [12,13] and shaping [14], while the aggregate can also be strengthened or stripped by physical, chemical, and biological methods, including nano-modification methods, microbial mineralization, and deposition methods, which can decrease the variability of RAC. However, these methods cannot be applied extensively and take away the variability at present. Therefore, the reliability analysis is very important for RAC considering its variability, which will also influence the design of RAC structures.

Compared with a NAC structure, the short-term and long-term behaviors of RAC structures are different. Research shows that [15,16] under compression, tension, or other loading conditions, the constitutive relationship curve of RAC with a high replacement ratio extremely differs from that of NAC; moreover, the peak strain is larger under compression. For RAC components, existing research includes the influence of coarse aggregate replacement ratio and the response of structures under static or seismic loading. The mechanical and seismic behaviors of reinforced RAC components are found to be inferior to those of NAC components with the same reinforcements [17]. However, the behavior of RAC components can be rendered equivalent to or even better than those of NAC through reasonable design so that they can be used in actual projects [18]. However, the shear resistance of RAC is a bit lower than that of NAC; it decreases by 6%–30% when the recycled coarse aggregate (RCA) replacement ratio is 100%. Further, the ductility of RAC columns is lower than that of NAC columns. Remarkably, RAC has better damping properties and high-temperature resistance than those NAC with the same water–binder ratio [19,20]. The long-term behavior of RAC components and structures compared with that of NAC is inferior. Nevertheless, it can be improved by applying appropriate structural measures.

Researchers have conducted lots of excellent work on the variability and reliability analysis of RAC structures. Pacheco and de Brito [21] and Pacheco et al. [22] found that one of the main reasons for skepticism towards RAC was the perceived notion that the heterogeneity of recycled aggregates might increase the uncertainty of the behavior of concrete, the structural reliability of RAC was the new trend in eco-efficient and recycled concrete. The determination of design parameters for RAC was important, Silva et al. [23] presented the relationship between the modulus of elasticity and compressive strength of RAC, which showed the loss of modulus of elasticity based on quality and replacement level of recycled aggregates. In the design of RAC structures, Breccolotti and Materazzi [24] and Pacheco et al. [25] studied the structural reliability of the bond between reinforcing steel bar and RAC, a partial factor could be determined so that the probability of failure of the bond length design of RAC could be equivalent to that of NAC. For the components, Breccolotti and Materazzi [26] studied the structural reliability of RAC columns; Silva and de Brito [27] proposed the design method of reinforced RAC slabs. Many researchers, including the authors of this investigation, analyzed the reliability of the flexural capacity of RAC beams, while that of the shear capacity of RAC beams was studied in the past few years. Pacheco et al. [22], Ju et al. [28], and Sunayana and Barai [29], established the database for RAC beams with and without shear reinforcement and proposed its safety margin or partial factor based on reliability

analysis. As for the durability of RAC components, Albuquerque et al. [30] and Faleschini et al. [31] studied the reliability-based analysis of RAC under carbonation and recommended the concrete cover design of RAC through comparison to that of NAC. Dehvari et al. [32] put forward the limited replacement ratio of RCA in a chloride ion environment through reliability-based design optimization. Cao et al. [33] and Li et al. [34] also studied the sulfate attack resistance of RAC based on reliability analysis.

Above all, the strength and variability of RAC materials differ from those of NAC because of the initial defects, waste material sources, and replacement ratio of recycled aggregates. Consequently, structural design calculations are expected to be inaccurate and can cause safety problems if the design method of NAC is directly applied without any modifications. The main difference between RAC and NAC structures can be determined if a unified design theory is established to benefit application and development. Moreover, the design method and design software of RAC could be unified with the existing NAC structural design. This can promote the engineering application of RAC because it can offer convenience to designers and manufacturers. Accordingly, the unified design theory of RAC and NAC structures has considerable theoretical and engineering significance.

Against this background, this paper mainly introduces the work of the authors' research group on the unified design theory of RAC and NAC, which aims to provide an analytical method that may be widely applicable. It mainly expounds on the unified method of structural resistance based on reliability; preliminarily discussions cover structural resistance based on time-dependent reliability. The development of the unified design theory of RAC and NAC components not only has engineering application significance but can also supplement and expand the design theory of NAC structures.

## 2. Determination of RAC strength

### 2.1. Representative value of compressive strength

#### 2.1.1. Coefficients of variation of compressive strength

The statistical parameters of component resistance can be determined by analyzing the strength of RAC when only limited test results on components are available; this is because strength is directly related to the bearing capacity of the components. At the same water–binder ratio, the mean strength of RAC is always lower than that of NAC [35–39]. This is mainly due to the inferior interfacial transition zones in RAC that cause different failure modes under compression [37]. The compressive strengths and the coefficient of variation (COV) of RAC with different replacement ratios based on reports in the literature [9,24,26,39–41] are presented in Fig. 1, in which the strength ratios and the COV ratios of RAC and NAC are provided. These data are collected from different countries and regions, including China, Spain, Portugal, and Italy; therefore, the properties of recycled aggregates are different.

The strength ratio of RAC to NAC is observed to decrease with an increasing replacement ratio (Fig. 1(a)), and the relationship between the COV and replacement ratio shows an increasing trend (Fig. 1(b)). From the trend line, when the replacement ratio of RCA is 100%, the compressive strength of RAC is decreased by approximately 10.0% and the COV is increased by approximately 20.0%.

#### 2.1.2. Compressive strength

The determination of the RAC strength should satisfy the requirements and corresponding material partial safety factors in the existing design codes, to ensure that the reliability of NAC and RAC structures reaches the same level. For NAC, the Chinese code GB 50010–2010 [42] stipulates the values of compressive

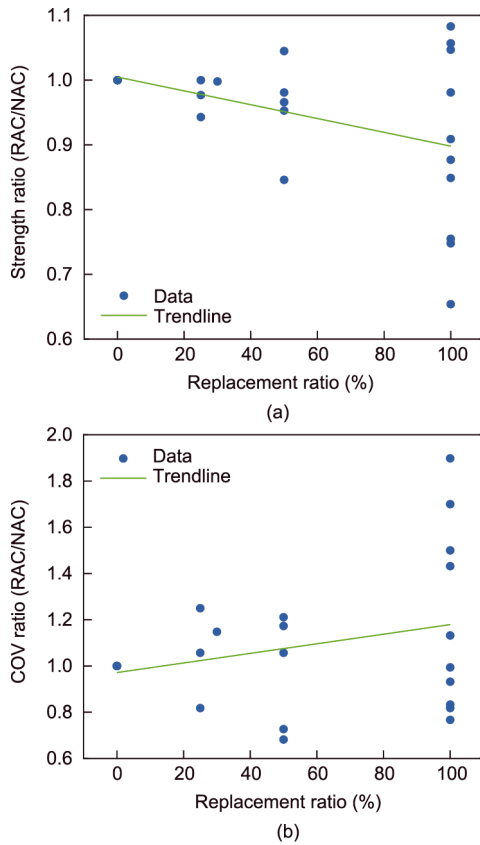


Fig. 1. The relationship between the replacement ratio and (a) the compressive strength ratio and (b) the COV ratio (RAC/NAC).

strength (including the mean, standard, and design strengths); the relationship among these values is also specified. The guaranteed standard strength of NAC is 95%, and the design strength is equal to the ratio of the standard strength to the partial safety factor. The material partial safety factors were obtained from engineering experience and reliability analysis; the partial safety factor of NAC was taken as 1.40.

In terms of the relationship of strength values, Xiao [43] conducted studies showing that the ratio of the axial compressive strength of RAC to the cubic compressive strength increased by approximately 8% compared with NAC, and concluded that the same strength conversion relationship can be used for RAC and NAC.

From the perspective of a unified strength value, the definition of standard and design strengths should be similar for NAC and RAC, and the COV of the RAC strength may be fully considered. For example, in the mix design of RAC, the standard deviation is 6.0 MPa (5.0 MPa for NAC); accordingly, the value of the partial safety factor of RAC needs to exceed 1.40.

## 2.2. Representative value of tensile strength

### 2.2.1. COV of tensile strength

Fig. 2 summarizes the tensile strength of RAC used in different countries [24,40]. The trend lines indicate that the mean values of tensile strength of RAC are decreasing with the replacement ratio of recycled aggregates, while the COV of strength shows an increasing trend. The number of tests on the tensile strength is relatively low compared with that on the compressive strength of RAC mainly because the tensile strength test is relatively difficult to perform.

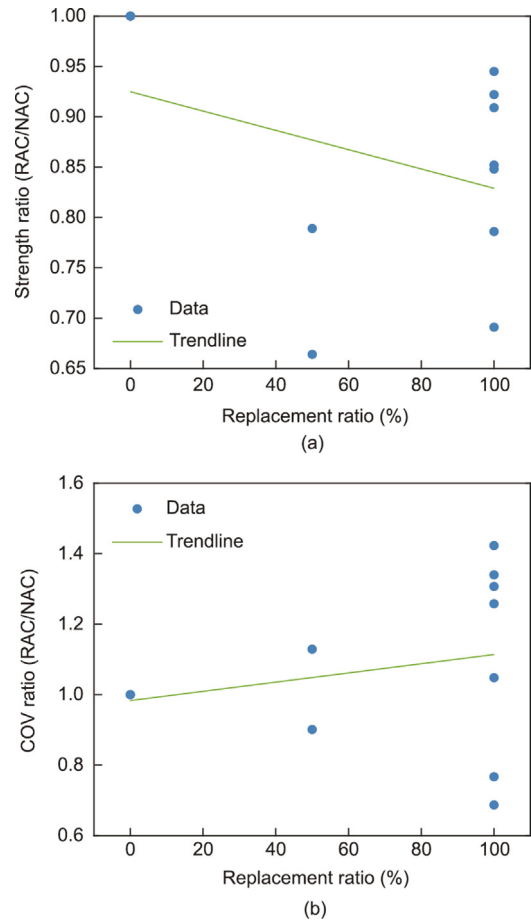


Fig. 2. The relationship between the replacement ratio and (a) the tensile strength ratio and (b) the COV ratio (RAC/NAC).

### 2.2.2. Tensile strength

The tensile strength of RAC is similar to the compressive strength, including the mean, standard, and design strengths, and these strength values conform to Chinese codes GB 50010–2010 [42] on NAC. The COV of RAC's tensile strength should also be considered, and the standard deviation and partial safety factor need to be increased correspondingly to ensure the rationality of the strength value.

The complex sources of recycled aggregates can increase the strength variability of RAC; this can in turn increase the COV of the bearing capacity of RAC components and reduce the reliability. To design the RAC components, the use of theoretical formulas similar to those of the NAC components is reasonable. The structural behavior and failure mechanism of RAC components are similar to those of NAC. The foregoing can facilitate the design, construction, and application of RAC structures as well as promote the unified design theory. Therefore, based on the reliability theory, the strength of RAC can be quantitatively determined. Then, the RAC components can be designed by modifying the existing design formula, finally satisfying the required reliability.

## 3. Constitutive relationship of RAC under uniaxial compression

### 3.1. Test methods

#### 3.1.1. Experimental information

The loading device is shown in Fig. 3. The specimen was a standard prism with dimensions of 150 mm × 150 mm × 300 mm.

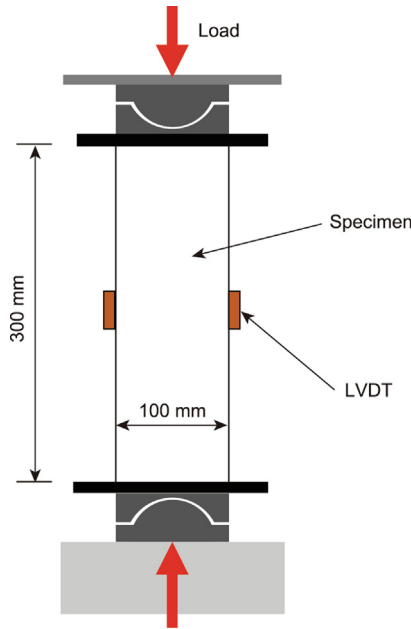


Fig. 3. Loading device. LVDT: linear variable differential transformer.

During the test, the load was applied at a strain rate of  $10^{-5} \text{ s}^{-1}$  which was regarded as quasi-static loading.

### 3.1.2. Stress–strain curves

The mean value and COV of stress–strain curves with different replacement ratios were calculated. The corresponding strain is 0–0.007, as shown in Fig. 4.

As shown in Fig. 4(a), the brittleness of RACs increases as the descending branch of the stress–strain curve becomes steeper compared with the curve of NAC. When the strain is less than 0.0062, the COV of the NAC stress shows an increasing trend with the strain, as shown in Fig. 4(b). For RACs, when the strain is less than 0.001, the COV of the RAC stress decreases with an increasing strain. Subsequently, the COV increases with the strain; however, no distinct trend has been observed for the specimen with a replacement ratio of 70%.

## 3.2. Stochastic constitutive model

### 3.2.1. Relationship among characteristic indices

The relationships between peak compressive stress ( $\sigma_{cp}$  (MPa)) and peak compressive strain ( $\epsilon_{cp} \times 10^{-3}$ ), between elastic modulus ( $E_c \times 10^4$  MPa) and standard cubic compressive strength ( $f_{cu,k}$  (MPa)), and between peak stress and shape factor ( $\alpha_c$ ) can be determined by Eqs. (1)–(3) which are from the Chinese code GB 50010–2010 [42], respectively:

$$\epsilon_{cp} = a_1 \cdot \sqrt{\sigma_{cp}} + b_1 \quad (1)$$

$$E_c = \frac{10}{a_2 + \frac{b_2}{f_{cu,k}}} \quad (2)$$

$$\alpha_c = a_3 \cdot \sigma_{cp}^{0.785} - b_3 \quad (3)$$

where  $a_1$ ,  $b_1$ ,  $a_2$ ,  $b_2$ ,  $a_3$ , and  $b_3$  are constants; for NAC, their values are 0.7, 0.172, 2.2, 34.7, 0.157, and 0.905, respectively.

The shape factor,  $\alpha_c$ , can be determined using Eq. (4), which relates to the ratio ( $\eta$ ) of the ultimate strain ( $\epsilon_{cu}$ ) to the peak strain ( $\epsilon_{cp}$ );  $\epsilon_{cu}$  is the corresponding strain when the stress drops to  $0.85\sigma_{cp}$ :

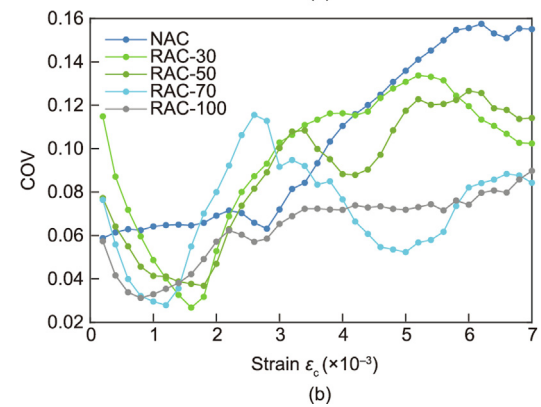
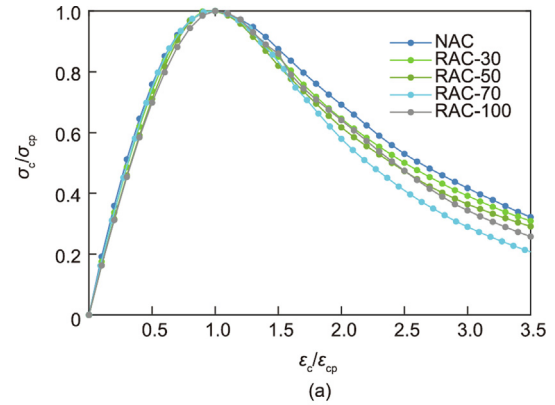


Fig. 4. (a) The normalized stress–strain curve and (b) the relationship between the COV and strain of the NAC and RAC with different replacement ratios.  $\sigma_c$ : compressive stress;  $\sigma_{cp}$ : peak compressive stress;  $\epsilon_c$ : compressive strain;  $\epsilon_{cp}$ : peak compressive strain. The number following RAC (30, 50, 70, 100) means the replacement ratio of RAC in percentage.

$$\alpha_c = \frac{\eta}{0.85 - \eta} - \eta \quad (4)$$

The relationships among the characteristic indices are shown in Figs. 5–7 where the test results are divided into three parts according to the specimen age (28, 56, and 150 days). The modified relations for RAC are developed with the test results both by the authors and the experimental data in the literature [16]. A total of 115 specimens are considered, including both prisms and cylinders, and these data are collected from eight references covering different countries and regions (the mainland of China, Spain, Brazil, Hong Kong of China, and Italy). The sources of recycled aggregates were various, and they were collected from the runway of an airport, real demolition waste of structural concrete, and specimens

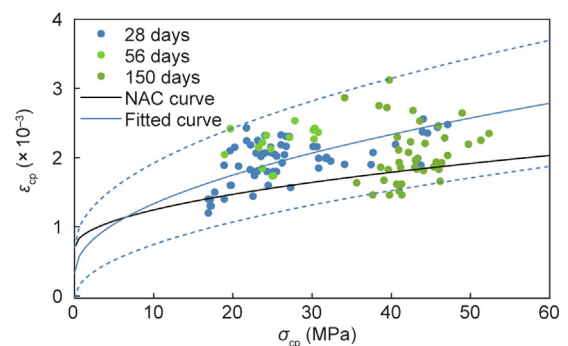


Fig. 5. Relation of peak stress and peak strain. The dotted line means the 95% confidence interval. Reproduced from Ref. [16] with permission.

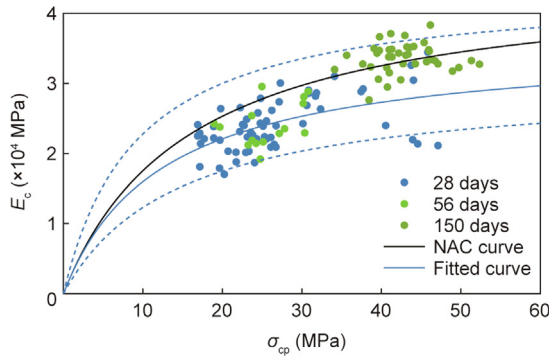


Fig. 6. Relation of elastic modulus and peak stress. The dotted line means the 95% confidence interval. Reproduced from Ref. [16] with permission.

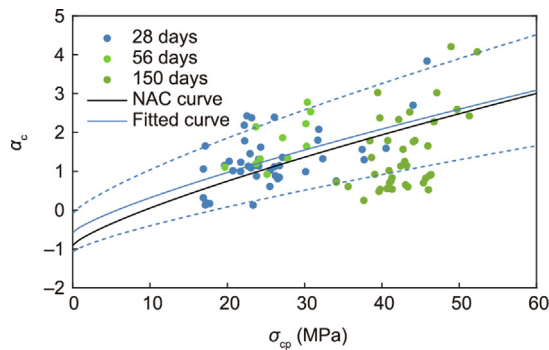


Fig. 7. Relation of shape factor and peak stress. The dotted line means the 95% confidence interval. Reproduced from Ref. [16] with permission.

crushed in compression tests in a concrete testing laboratory, and so forth. Therefore, the properties of the recycled aggregates were different, such as the water absorption (3.20%–9.25%), apparent density (2381–2525 kg·m<sup>-3</sup>), and crushing index (15.2%–19.5%).

The coefficient of determination ( $R^2$ ) values of the fitted lines for the relation between the peak stress and peak strain, peak stress, and elastic modulus, and peak stress and shape parameter are 0.58, 0.59, and 0.29, respectively. The  $R^2$  values for the relations between the characteristic parameters indicate that the variability cannot be ignored, therefore, the stress–strain relationship of RAC should be modified based on the existing models and the collected experimental data. Further related studies are still needed to evaluate the variability and the stress–strain relationship models.

By fitting the curves, the age of concrete was found to significantly affect the elastic modulus of RAC; however, its effect on the peak strain was less. Cement continues to hydrate with the concrete ages, improving both the elastic modulus and strength. When the strengths are the same, the elastic modulus of RAC is smaller than that of NAC; however, its peak strain and shape coefficient are larger.

### 3.2.2. Modified relationships

Based on the relationship among the characteristic indices, the RAC model is obtained by modifying the Chinese code models given by Eqs. (1)–(3). The stress–strain curves of RAC and NAC with different strengths are obtained, as shown in Fig. 8. In Fig. 8(a), the peak strain and elastic modulus of RAC and NAC increase with the strength level; however, the descending stage of the curves becomes steep. The descending branch of the curve of RAC compared with that of NAC becomes considerably steep when its strength increases from 20 to 45 MPa, indicating that its brittleness increases, as can be observed in Fig. 8(b). Compared with those of

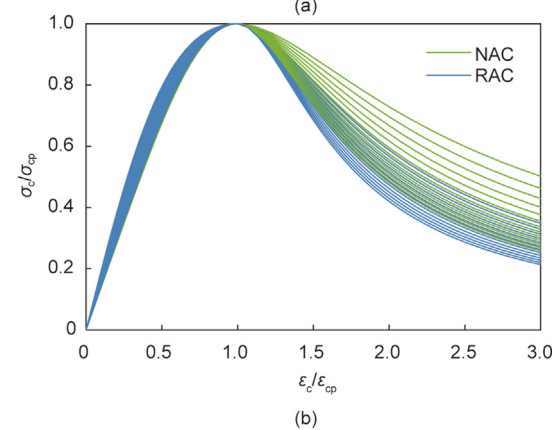
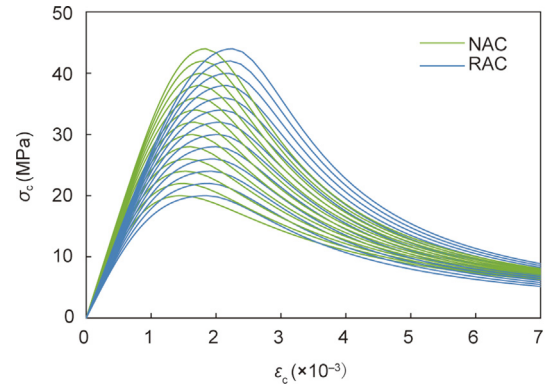


Fig. 8. Comparison of NAC and RAC at different strength levels: the main stress-strain curves (a) with and (b) without normalized.

NAC, the elastic modulus of RAC is 27 110 MPa (which was 17% lower), and its peak strain is 0.0022 when the peak stress is 40 MPa (which was 23% higher). The shape factors of RAC and NAC given by the descending branch are 2.489 and 1.936, respectively.

The constitutive models of RAC and NAC under uniaxial compression can have a similar mathematical expression (i.e., Eq. (5)); in which the definition and expression of the parameters  $\rho_c$  and  $m$  are the same:  $\rho_c = \frac{\sigma_{cp}}{E_c \varepsilon_{cp}}$ ;  $m = \frac{E_c \varepsilon_{cp}}{E_c \varepsilon_{cp} - \sigma_{cp}}$ ; and  $d_c$  is the damage factor (see Eq. (6)). The difference is that in the RAC model, the relationship among the characteristic indices is determined through collected data, and the probability distribution of stress is tested. At a given strain, the corresponding stress follows a normal distribution.

$$\sigma_c = (1 - d_c) E_c \varepsilon_c \tag{5}$$

$$d_c = \begin{cases} 1 - \frac{\rho_c m}{m-1+\eta^m} & 0 \leq \eta < 1 \\ 1 - \frac{\rho_c}{\alpha_c (\eta-1)^2 + \eta} & \eta > 1 \end{cases} \tag{6}$$

where the shape factor,  $\alpha_c$ , of the descending branch can be determined using Eq. (7):

$$\alpha_c = 0.151 \sigma_{cp}^{0.785} + 0.182 \tag{7}$$

## 4. Bearing capacity of RAC beams based on reliability analysis

### 4.1. Partial safety factor of RAC

#### 4.1.1. Calculation process

The RAC beam is presented as a calculation example; the factors considered are: load type (constant load and live load), ratio of

constant load to live load (0.25, 0.5, 1.0, 1.5, and 2.0), concrete grade (C30 and C40), steel grade (hot rolled ribbed bars (HRB) with yield strength of 335 and 400 MPa, HRB335 and HRB400), and four reinforcement ratios ( $\rho$ ).

The standard, mean, and design strengths of RAC and NAC remained the same (the strengths of the NAC beam are used as a reference). In calculating the RAC partial safety factor, the COV of its strength was set to 8.0%–20.0%.

#### 4.1.2. Determination of partial safety factor of RAC

When the standard strength of RAC remains the same as that of NAC, the partial safety factors of RAC, including those of concrete grades C30 and C40, are calculated. The calculation results are grouped according to the reinforcement ratio, and a curve with a 95% guarantee ratio is given, as shown in Fig. 9.

As shown in Fig. 9, when the standard compressive strengths are the same, the partial safety factors of RAC can decrease when the COV of its compressive strength increases. This is mainly because RAC's mean compressive strength increases when a high COV is adopted, improving the reliability index of the RAC beams. When the COV of its compressive strength exceeds 0.13 (NAC C30) or 0.10 (NAC C40), the calculated values of the partial safety factors of RAC reach the maximum value at the maximum reinforcement ratio. The COV of its compressive strength was assumed to increase by 10% with the same standard strength. The partial safety factors of C30 and C40 RAC were determined to be 1.45 with a 95% guarantee because of the relatively high variability.

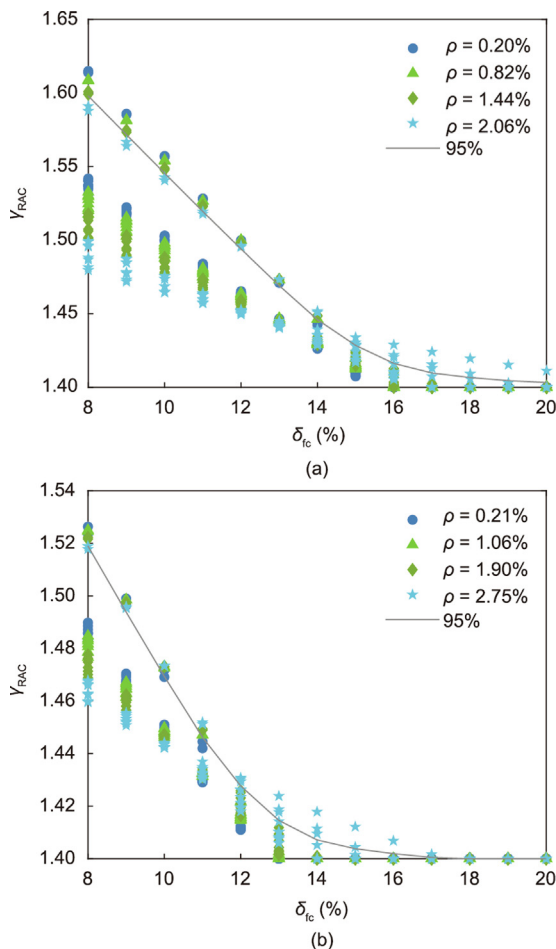


Fig. 9. Partial safety factors of RAC: (a) C30 and (b) C40.  $\gamma_{RAC}$ : partial safety factor of RAC;  $\delta_{fc}$ : COV of compressive strength.

If the mean strengths of NAC and RAC are the same, the reliability of the RAC beams can be improved by increasing the reinforcement ratio, implying a low demand for the mix strength of RAC. For the same standard strength, increasing the reinforcement ratio is necessary to improve the reliability when the COV is small. For the same design strength, the mix strength of RAC should be improved. This can be achieved by controlling the quality of recycled aggregates and optimizing the mix design of RAC.

#### 4.2. Minimum reinforcement/stirrup ratio of RAC beams

##### 4.2.1. Minimum reinforcement ratio

The minimum reinforcement ratio ( $\rho$ ) of RAC beams can be expressed by Eq. (8), which is the same as that of NAC:

$$\rho_{R,min} = \eta_b \frac{f_t}{f_y} \tag{8}$$

For NAC,  $\eta_b = 0.45$ , which is the reinforcement ratio coefficient;  $f_y$  and  $f_t$  are the design values of the tensile strength of the longitudinal reinforcement and RAC, respectively.

The minimum reinforcement ratio of RAC beams is determined by keeping the reliability index the same as that of NAC beams; this method is similar to the calculation method for RAC partial safety factors. During the calculation process, the strength grades of RAC were C30 and C40, and those of the steel bars were HRB335 and HRB400. The relationship between  $\eta_b$  and COV ( $\delta_{fc}$ ) is shown in Fig. 10, and  $R^2$  is 0.98.

As shown in Fig. 10, the minimum reinforcement ratio of the RAC beams increases exponentially with the increase of COV of compressive strength. The ratio slightly improves compared with that of the NAC beams because the influence of the COV of strength is limited by the contribution of reinforcement. Therefore, when the COV increases, the decrease in the reliability index is limited. Moreover, only a small amount of reinforcement is required for the reliability index of the RAC beams to attain the index level of the NAC beams. In summary,  $\eta_b$  can be considered as 0.47, as shown in Fig. 10.

##### 4.2.2. Minimum stirrup ratio

The minimum stirrup ratio of the RAC beams ( $\rho_{R,sv,min}$ ) can be expressed by Eq. (9), which is similar to that of NAC beams:

$$\rho_{R,sv,min} = \eta_s \frac{f_t}{f_y} \tag{9}$$

where  $\eta_s$  is the stirrup ratio coefficient; for NAC,  $\eta_s = 0.24$ .

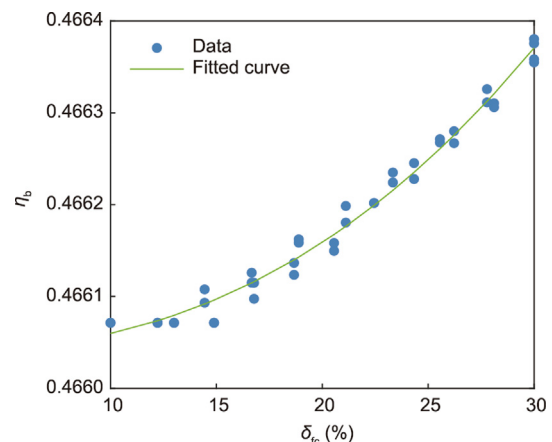


Fig. 10. Minimum reinforcement ratio coefficient of RAC beams.

Similar to the calculation method of the minimum reinforcement ratio ( $\rho$ ), in the computation, the chosen concrete strength grades were C30 and C40, and those of the steel bars were hot-rolled plain bar (HPB) with the yield strength of 300 MPa (HPB300) and HRB335. The relationship between  $\eta_s$  and the COV of tensile strength ( $\delta_{ft}$ ) is shown in Fig. 11, and  $R^2$  is 0.97.

This figure indicates that the minimum stirrup ratio coefficient,  $\eta_s$ , increases with the increase of COV of tensile strength. When the strength grade is C30 with a COV of 15% and the stirrup is HRB335, the  $\eta_s$  is 0.261, and the minimum stirrup ratio of the RAC beams increases by 8.7% compared with that of the NAC beams. When the COV increases to 20%, the minimum stirrup ratio increases by 36.3%, indicating that when the stirrup ratio is small, the COV of the tensile strength significantly influences the COV of the shear capacity, reducing the reliability index of the beams. Therefore, increasing the stirrup ratio is necessary to ensure that its reliability satisfies the foregoing requirements. Generally, when the COV of strength is controlled within 15%,  $\eta_s$  can be taken as 0.28.

### 4.3. Bearing capacity of components

#### 4.3.1. Flexural capacity

The design value of the bending moment,  $M$ , of the beams can be satisfied by Eqs. (10) and (11), as follows:

$$M \leq \alpha_1 f_c b x \left( h_0 - \frac{x}{2} \right) \tag{10}$$

$$\alpha_1 f_c b x = f_y A_s \tag{11}$$

where  $\alpha_1$ ,  $f_c$ , and  $x$  have the same definitions as those for NAC;  $\alpha_1$  is equal to 1.0;  $f_c$  is the design strength value;  $x \leq \xi_b h_0$  and  $\xi_b = \beta_1 / [1 + f_y / (E_s \varepsilon_{cu})]$ , in which  $\beta_1$  is the coefficient (0.78);  $\varepsilon_{cu}$  is the ultimate strain of concrete;  $E_s$  is the steel bar's elastic modulus;  $b$  and  $h_0$  are the width and effective height of the cross-section, respectively; and  $A_s$  and  $f_y$  are the cross-sectional area and design tensile strength of the longitudinal steel bars, respectively.

#### 4.3.2. Shear capacity

The shear force,  $V$ , of RAC beams can be satisfied by Eq. (12):

$$V \leq 0.9 \alpha_{cv} f_t b h_0 + A_{sv} f_{yv} \frac{h_0}{s} \tag{12}$$

where 0.9 is the modified reliability coefficient of RAC; parameter of shear capacity  $\alpha_{cv}$  is 0.7 for common concrete beams and  $\frac{1.75}{\lambda+1}$  for beams with a concentrated load ( $\lambda$  is the shear span ratio);  $A_{sv}$

and  $f_{yv}$  are the cross-sectional area and design tensile strength of stirrups, respectively; and  $s$  is the stirrup spacing.

The partial safety factor, minimum reinforcement ratio, stirrup ratio, and shear bearing capacity of RAC were obtained based on reliability analysis. The component shear design methods of NAC and RAC can be unified. Values should be modified after fully considering the characteristics of RAC to realize the unified design theory of NAC and RAC components. The foregoing results provide theoretical support for the revision of the Chinese code DG/TJ 08–2018–2020 [2].

## 5. Preliminary study on time-dependent reliability of RAC components

The unified design formula of the RAC components can be determined by reliability analysis. Regarding the durability problem, the current specification has certain requirements regarding concrete strength grade and minimum thickness of the concrete cover. Preliminary research has been conducted on the time-dependent behavior of RAC components. It mainly includes the time-dependent strength of NAC and RAC, carbonation behavior, corrosion of steel reinforcement, and time-dependent reliability analysis. The foregoing is considered to establish the foundation for the design of NAC and RAC components based on the time-dependent reliability.

The durability problem of concrete structures originates from the deterioration of concrete or steel reinforcement that can be caused by environmental conditions. The RAC time-dependent strength data were collected from Ref. [44] and the time-dependent strength model of NAC. Based on these values, the prediction results of the RAC time-dependent strength and corresponding COV were obtained by preliminary fitting. The development trend of the RAC time-dependent strength is found to be consistent with that of NAC. The short-term strength of RAC is relatively low, but the COV of its compressive strength is a bit high. As the service time progresses, the absolute difference between them might increase. The COV of the strengths of RAC and NAC first decreased and then gradually increased.

Research on the carbonation of RAC has been conducted, and different prediction models for carbonation depth have been put forward. The authors proposed a revised carbonation depth prediction model for RAC based on existing models [45], as given in Eq. (13). This model considers water absorption, temperature, relative humidity, curing time, water–cement ratio, 28-day compressive strength, CO<sub>2</sub> concentration, and carbonation time:

$$x_c(t) = 104k_A \cdot \sqrt[4]{T} \cdot k_e \cdot \sqrt{\frac{k_c \cdot W}{f_c^3 \cdot C}} \cdot k_{CO_2} \cdot \sqrt{t} \tag{13}$$

where  $x_c(t)$  is the carbonation depth at service time  $t$ ;  $k_A$  is the water absorption ratio parameter of aggregates;  $T$  is the temperature ( $^{\circ}C$ );  $k_e$  is the environmental function ( $k_e = RH^{1.5}(1 - RH)$ );  $RH$  is the relative humidity;  $k_c$  is the execution transfer parameter;  $W$  and  $C$  are the content of water and cement in concrete ( $kg \cdot m^{-3}$ ), respectively;  $k_{CO_2}$  is the CO<sub>2</sub> concentration coefficient;  $k_{CO_2} = \sqrt{\frac{C_0}{0.03}}$ ; and  $C_0$  is the CO<sub>2</sub> concentration by volume (%).

The modified model could effectively predict the carbonation depth which is verified by using ten years of carbonation data [44]. The prediction results show that the carbonation depths of NAC and RAC can increase with time. For RAC, the carbonation depth can also increase when the RCA replacement ratio increases.

Concrete carbonation can reduce the pH value of the concrete, leading to steel reinforcement corrosion due to environmental effects. The critical expansion force is modified by considering different yield criteria for the plastic properties of concrete. The

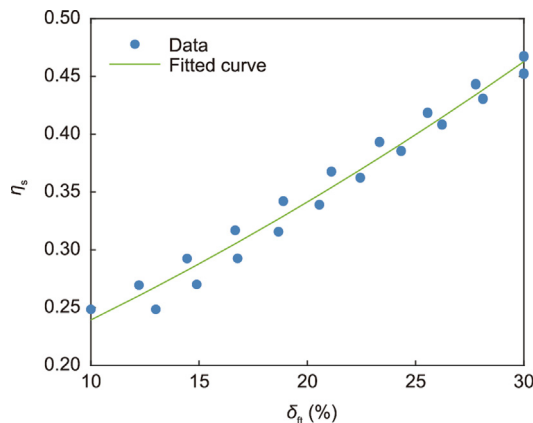


Fig. 11. Minimum stirrup ratio coefficient of RAC beams.  $\delta_{ft}$ : COV of the tensile strength.

relationship between this force and the parameters is established based on the elastic–plastic analysis.

Upon steel reinforcement corrosion, the crack development initiates within the concrete cover when the expansion force increases. A concrete ring with partial cracks separates into plastic and elastic zones whose boundary conditions can be established. The calculation process for the critical sectional loss rate of reinforcements is obtained by considering the boundary and deformation coordination conditions [46].

During the calculation process, RAC and NAC were not differentiated. Therefore, the foregoing calculation method and unified model are feasible for both models, and the model is verified by many experimental results [47].

Based on the RAC time-dependent strength, carbonation depth, and expansion force model of the corroded steel reinforcement, the time-dependent bearing capacity of beams can be obtained through numerical simulation using the OpenSees software (USA). The stochastic time-dependent constitutive relationships between RAC and reinforcement were considered. The bearing capacity of RAC beams at different ages was calculated. The fitted curve and calculated data are compared, as shown in Figs. 12 and 13; the  $R^2$  values are 0.983 and 0.859, respectively. This means that the data of the RAC beams can be well described by the established models.

The decrease rate of the resistance can increase with the service time, as displayed in Fig. 12. This is mainly because the sectional loss rate of the steel reinforcement increases gradually with the service time. In addition, the RAC time-dependent strength decreases after the peak strength; this was the reason for the reduction in the mean value of the resistance. The standard deviation of the resistance can increase gradually with the service time, as shown in Fig. 13. This mainly occurred because the COVs of the strengths of both reinforcement and RAC increased. In conclusion, with increasing service time, the mean value of time-dependent resistance gradually decreased, whereas its COV increased.

The hypothesis was tested based on the established time-dependent beam resistance model. The results show that during service, the resistance is a lognormal random process as it follows a lognormal distribution at a given time. The degradation of resistance can decrease the reliability index in the design reference period and affect the structural safety. Therefore, conducting a time-dependent modification of the partial safety factor of RAC is necessary; this is also a key problem requiring further research.

Consider the RAC beam as an example. Time-dependent reliability was obtained by analyzing the time-dependent strength, carbonation depth, expansion of steel reinforcement, and time-dependent resistance. Note that the prediction results of the time-dependent strength and carbonation depth of RAC are mainly obtained using only the 10-year test data. Based on the NAC models, the unified prediction models of time-dependent strength, carbonation depth, and expansion force of the corroded steel reinforcement were obtained. However, the long-term test data remain insufficient, and more engineering data are required to modify the model. The time-dependent resistance of the beams was mainly obtained by numerical simulation. Further modification by relevant experiments on the durability and monitoring of practical structures is necessary. Furthermore, the time-dependent reliability of other RAC members must be investigated to determine a reasonable design method for RAC components based on time-dependent reliability. In the context of the national strategy on low-carbon emissions, the time-dependent reliability design of RAC structures should consider future climate change and follow the principles of safety and low carbon emissions.

In this section, the authors aimed to find a design method for RAC components in which the properties, particularly the durability of RAC should be reasonably considered. Therefore, the authors

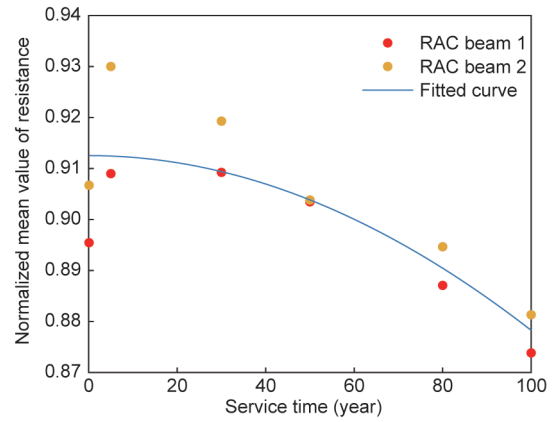


Fig. 12. Fitting results of mean resistance.

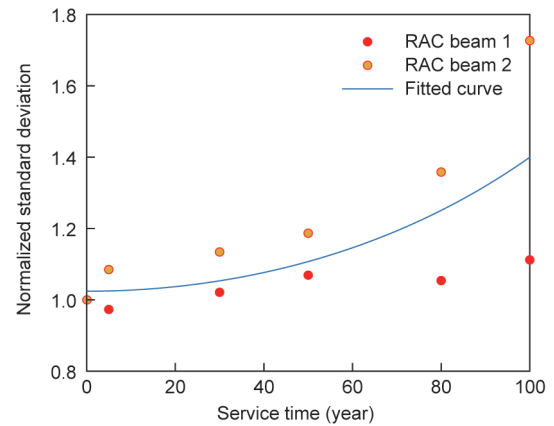
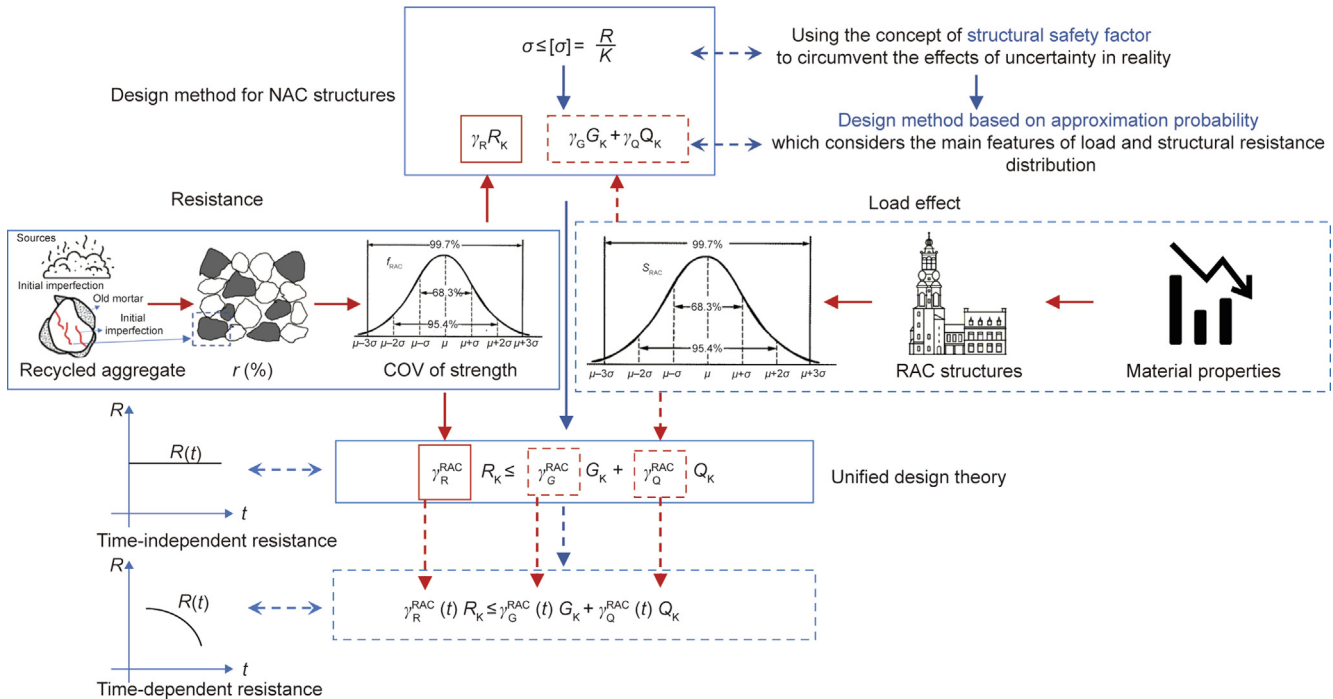


Fig. 13. Fitting results of standard deviation.

investigated the long-term strength and carbonation of RAC, corrosion of steel reinforcement in RAC, and flexural resistance of RAC beams, and calculated the time-dependent reliability of RAC components. The results indicate that the time-dependent reliability of RAC components can be evaluated and can provide useful information in the design of RAC components. Assumptions were made in these investigations, such as the uniform corrosion of steel reinforcement, and the accelerated experimental results were used to evaluate the long-term performance of RAC components. In the next step, the authors will collect the *in-situ* structural data and evaluate the structural behavior of RAC components, in which the models will be updated and calibrated. Finally, the partial safety factor of RAC which can reflect the difference in performance between RAC and normal concrete will be proposed based on the time-dependent reliability analysis.

Above all, to establish a unified design theory, the following problems need to be considered. The strength of RAC can be related to that of NAC through the correlation function of the replacement ratio. However, the relationship between its variability and replacement ratio is difficult to determine; the key problem is determining the design parameters. To achieve a unified design method, the target reliability of RAC and NAC structures must be consistent. Further, the characteristics of the RAC structure must be reflected based on the NAC design method, which can be applied to existing design software. The concept of the unified design theory is summarized and illustrated in Fig. 14. Note that the load effect of RAC has certain differences compared with that of NAC and must be studied in the future. For example, owing to the difference in thermal and damping parameters, the structural



**Fig. 14.** Unified design theory of RAC and NAC structures.  $\sigma$ : stress;  $[\sigma]$ : critical stress;  $R$ : resistance;  $K$ : structural safety factor;  $\gamma_R$ : partial safety factor of resistance;  $R_K$ : standard value of resistance;  $\gamma_G$ : partial safety factor of constant load effects;  $G_K$ : standard value of constant load effects;  $\gamma_Q$ : partial safety factor of live load effects;  $Q_K$ : standard value of live load effects;  $r$ : replacement ratio of RCA;  $f_{RAC}$ : strength of RAC;  $S_{RAC}$ : load effects of RAC components;  $R(t)$ : time-dependent resistants;  $t$ : service time;  $\gamma_R^{RAC}$ : partial safety factor of resistance for RAC;  $\gamma_G^{RAC}$ : partial safety factor of constant load effects for RAC;  $\gamma_Q^{RAC}$ : partial safety factor of live load effects for RAC;  $\gamma_R^{RAC}(t)$ : time-dependent partial safety factor of resistance for RAC;  $\gamma_G^{RAC}(t)$ : time-dependent partial safety factor of constant load effects for RAC;  $\gamma_Q^{RAC}(t)$ : time-dependent partial safety factor of live load effects for RAC.

action effects of RAC differ under earthquake forces and varying temperatures.

## 6. Concluding remarks

### 6.1. Conclusions

Based on the requirements for the unified design of NAC and RAC components, the strength value, compression constitutive relationship, and unified design method based on the reliability theory are examined in this study. The following conclusions can be drawn:

(1) The COV of RAC strength is a bit higher compared with that of NAC strength. This is mainly due to the complex sources, randomization, and quality of the old mortar attached to recycled aggregates. The definition and determination method of the representative compressive and tensile strength values of RAC are consistent with those of NAC. Moreover, modifying the partial safety factor of RAC is necessary because the variation in strength can increase its standard deviation, consequently affecting the representative strength values.

(2) Based on the constitutive model for NAC, a unified model has been derived by modifying the relationships among the characteristic indices. The elastic modulus of RAC is lower than that of NAC, and the decreasing branch of its stress–strain curve is steeper, indicating higher brittleness. A random distribution test shows that stress follows a normal distribution at a given strain, laying the foundation for the nonlinear analysis of RAC structures.

(3) Based on the reliability analysis, the partial safety factors of RAC, minimum steel reinforcement and stirrup ratios, and bearing capacity design formula of RAC components can be determined. The COV of the RAC mechanical properties is higher than that of NAC; the foregoing increases the partial safety factors, minimum reinforcement ratio, and stirrup ratio of RAC beams. Modified reliability factors for the RAC components are proposed to realize a

unified design formula and establish a convenient theoretical basis for the computer-aided design of RAC structures.

(4) The strength development, carbonation of concrete, and corrosion of the steel reinforcement are important factors affecting the time-dependent bearing capacity of concrete structures. The mean value of the bearing capacity decreases with the service time, whereas the COV gradually increased, resulting in a decrease in the time-dependent reliability index. The current design method is mainly based on the reliability theory, and structural measures are implemented to ensure structural safety during service life. A unified design method based on time-dependent reliability can improve the future design theory of concrete structures.

### 6.2. Research opportunities

Future research can mainly focus on the following aspects.

(1) Long-term behavior of RAC: Considering the variability and durability of RAC, its long-term behavior, and corresponding modification methods should be thoroughly studied based on multi-scale analysis to ensure safety.

(2) Performance monitoring of RAC components and structures during service time: Field accurate data on the mechanical behavior of RAC components obtained from practical engineering are relevant for evaluating structural responses. Moreover, they can provide feedback and verify the design method of RAC structures.

(3) Carbon emissions of RAC: Analyzing the carbon emission factors and compiling carbon emission data of RAC are necessary to further improve the unified design method in terms of sustainability.

## Acknowledgments

The authors wish to acknowledge the financial support from the Distinguished Young Scholars of China by the National Natural

Science Foundation of China (51325802) and the National Natural Science Foundation of China (51178340, 52078358, and 52008304).

### Compliance with ethics guidelines

Jianzhuang Xiao, Kaijian Zhang, Tao Ding, Qingtian Zhang, and Xuwen Xiao declare that they have no conflicts of interest or financial conflicts to disclose.

### References

- [1] Bendixen M, Best J, Hackney C, Iversen LL. Time is running out for sand. *Nature* 2019;571(7763):29–31.
- [2] Construction SR, Committee M. DG/TJ 08–2018–2020: Technical standard on the application of recycled aggregate concrete. Chinese standard. Shanghai: Tongji University Press; 2020. Chinese.
- [3] Marinković SB, Malešev M, Ignjatović I. Life cycle assessment (LCA) of concrete made using recycled concrete or natural aggregates. In: Pacheco-Torgal F, Cabeza LF, de Magalhães A, editors. Eco-efficient construction and building materials. New Delhi: Woodhead Publishing; 2014. p. 239–66.
- [4] Duan Z, Hou S, Xiao J, Li B. Study on the essential properties of recycled powders from construction and demolition waste. *J Clean Prod* 2020;253:119865.
- [5] de Oliveira MB, Vazquez E. The influence of retained moisture in aggregates from recycling on the properties of newly hardened concrete. *Waste Manage* 1996;16(1–3):113–7.
- [6] Poon CS, Shui ZH, Lam L. Effect of microstructure of ITZ on compressive strength of concrete prepared with recycled aggregates. *Constr Build Mater* 2004;18(6):461–8.
- [7] Adessina A, Ben Fraj A, Barthélémy J, Chateau C, Garnier D. Experimental and micromechanical investigation on the mechanical and durability properties of recycled aggregates concrete. *Cement Concr Res* 2019;126:105900.
- [8] Bravo M, de Brito J, Pontes J, Evangelista L. Mechanical performance of concrete made with aggregates from construction and demolition waste recycling plants. *J Clean Prod* 2015;99:59–74.
- [9] Etxeberria M, Vázquez E, Mari A, Barra M. Influence of amount of recycled coarse aggregates and production process on properties of recycled aggregate concrete. *Cement Concr Res* 2007;37(5):735–42.
- [10] Thomas C, de Brito J, Cimentada A, Sainz-Aja JA. Macro- and micro-properties of multi-recycled aggregate concrete. *J Clean Prod* 2020;245:118843.
- [11] Ozbakkaloglu T, Gholampour A, Xie TY. Mechanical and durability properties of recycled aggregate concrete: effect of recycled aggregate properties and content. *J Mater Civ Eng* 2018;30(2):04017275.
- [12] Shi C, Li Y, Zhang J, Li W, Chong L, Xie Z. Performance enhancement of recycled concrete aggregate—a review. *J Clean Prod* 2016;112:466–72.
- [13] Kazmi SMS, Munir MJ, Wu Y, Patnaikuni I, Zhou Y, Xing F. Effect of recycled aggregate treatment techniques on the durability of concrete: a comparative evaluation. *Constr Build Mater* 2020;264:120284.
- [14] Song IH, Ryou JS. Hybrid techniques for quality improvement of recycled fine aggregate. *Constr Build Mater* 2014;72:56–64.
- [15] Xiao J, Li J, Zhang C. Mechanical properties of recycled aggregate concrete under uniaxial loading. *Cement Concr Res* 2005;35(6):1187–94.
- [16] Xiao JZ, Zhang KJ, Akbarnezhad A. Variability of stress-strain relationship for recycled aggregate concrete under uniaxial compression loading. *J Clean Prod* 2018;181:753–71.
- [17] Domínguez-Santos D, Letelier V, Muñoz P. Seismic capacity of 2- and 3-storey RC buildings with eco-concrete made by using residues for replacing natural aggregates. *J Build Eng* 2020;28:101086.
- [18] Al Mahmoud F, Boissiere R, Mercier C, Khelil A. Shear behavior of reinforced concrete beams made from recycled coarse and fine aggregates. *Structures* 2020;25:660–9.
- [19] Li T, Xiao J, Singh A. Influence of new-to-old concrete interface on the damping behavior of recycled aggregate concrete. *Struct Concr* 2021;22(5):3109–22.
- [20] Khan A, Aziz T, Fareed S, Xiao J. Behaviour and residual strength prediction of recycled aggregates concrete exposed to elevated temperatures. *Arab J Sci Eng* 2020;45(10):8241–53.
- [21] Pacheco J, de Brito J. Structural reliability of recycled aggregate concrete. In: de Brito J, Agrela F, editors. *New trends in eco-efficient and recycled concrete*. New Delhi: Woodhead Publishing; 2019. p. 541–72.
- [22] Pacheco J, de Brito J, Chastre C, Evangelista L. Eurocode shear design of coarse recycled aggregate concrete: reliability analysis and partial factor calibration. *Materials* 2021;14(15):4081.
- [23] Silva RV, de Brito J, Dhir RK. Establishing a relationship between modulus of elasticity and compressive strength of recycled aggregate concrete. *J Clean Prod* 2016;112:2171–86.
- [24] Breccolotti M, Materazzi AL. Structural reliability of bonding between steel rebars and recycled aggregate concrete. *Constr Build Mater* 2013;47:927–34.
- [25] Pacheco JN, de Brito J, Chastre C, Evangelista L. Bond of recycled coarse aggregate concrete: model uncertainty and reliability-based calibration of design equations. *Eng Struct* 2021;239:112290.
- [26] Breccolotti M, Materazzi AL. Structural reliability of eccentrically-loaded sections in RC columns made of recycled aggregate concrete. *Eng Struct* 2010;32(11):3704–12.
- [27] Silva RV, de Brito J. Reinforced recycled aggregate concrete slabs: structural design based on Eurocode 2. *Eng Struct* 2020;204:110047.
- [28] Ju H, Yerzhanov M, Serik A, Lee D, Kim JR. Statistical and reliability study on shear strength of recycled coarse aggregate reinforced concrete beams. *Materials* 2021;14(12):3321.
- [29] Sunayana S, Barai SV. Shear and serviceability reliability of recycled aggregate concrete beams. *ACI Struct J* 2021;118(2):225–36.
- [30] Albuquerque A, Pacheco J, de Brito J. Reliability-based recommendations for EN1992 carbonation cover design of concrete with coarse recycled concrete aggregates. *Struct Concr* 2022;23(3):1873–89.
- [31] Faleschini F, Zanini MA, Hofer L. Reliability-based analysis of recycled aggregate concrete under carbonation. *Adv Civ Eng* 2018;2018:1–11.
- [32] Dehvari AG, Miri M, Sohrabi MR. Reliability-based design optimization of recycled coarse aggregates used in corrosive environment. *J Mater Civ Eng* 2021;33(4):04021042.
- [33] Cao H, Zhao L, Lu C, Guan L, Qiao H, Li Q. Degradation resistance and reliability analysis of recycled aggregate concrete in a sulfate environment. *Adv Mater Sci Eng* 2020;2020:1–11.
- [34] Li J, Qiao H, Guan L, Zhu F. Sulfate attack resistance and reliability analysis of recycled aggregate concrete. *Emerg Mater Res* 2020;9(3):877–86.
- [35] Torben CH. Recycled aggregates and recycled aggregate concrete second state-of-the-art report developments 1945–1985. *Mater Struct* 1986;19:201–46.
- [36] Rahal K. Mechanical properties of concrete with recycled coarse aggregate. *Build Environ* 2007;42(1):407–15.
- [37] Watanabe T, Nishibata S, Hashimoto C, Ohtsu M. Compressive failure in concrete of recycled aggregate by acoustic emission. *Constr Build Mater* 2007;21(3):470–6.
- [38] Tabsh SW, Abdelfatah AS. Influence of recycled concrete aggregates on strength properties of concrete. *Constr Build Mater* 2009;23(2):1163–7.
- [39] Xiao ZJ, Li JB, Zhang C. On statistical characteristics of the compressive strength of recycled aggregate concrete. *Struct Concr* 2005;6(4):149–53.
- [40] Yuan B. On values of compressive strength and tensile strength of recycled aggregate concrete [dissertation]. Shanghai: Tongji University; 2007. Chinese.
- [41] Matias D, de Brito J, Rosa A, Pedro D. Mechanical properties of concrete produced with recycled coarse aggregates—influence of the use of superplasticizers. *Constr Build Mater* 2013;44:101–9.
- [42] Ministry of Housing and Urban–Rural Development of the People's Republic of China. GB 50010–2010: Code for design of concrete structures. Chinese standard. Beijing: China Architecture and Building Press; 2010. Chinese.
- [43] Xiao JZ. Recycled aggregate concrete structure. Berlin: Springer; 2018.
- [44] Kou S, Poon C. Long-term mechanical and durability properties of recycled aggregate concrete prepared with the incorporation of fly ash. *Cement Concr Compos* 2013;37:12–9.
- [45] Zhang KJ, Xiao JZ. Prediction model of carbonation depth for recycled aggregate concrete. *Cement Concr Compos* 2018;88:86–99.
- [46] Zhang KJ, Xiao JZ, Zhao YX, Zhang QT. Analytical model for critical corrosion level of reinforcements to cause the cracking of concrete cover. *Constr Build Mater* 2019;223:185–97.
- [47] Zhao Y, Yu J, Wu Y, Jin W. Critical thickness of rust layer at inner and out surface cracking of concrete cover in reinforced concrete structures. *Corros Sci* 2012;59:316–23.